

## Direct Measurements of Pore Fluid Density by Vibrating Tube Densimetry

Mirosław S. Gruszkiewicz,\* Gernot Rother, and David J. Wesolowski

Chemical Sciences Division, Oak Ridge National Laboratory, Oak Ridge, Tennessee 37831, United States

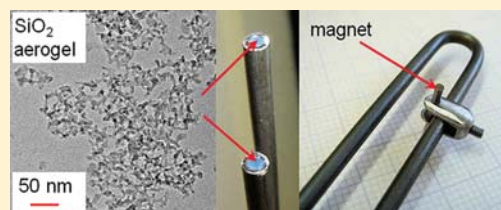
David R. Cole

School of Earth Sciences, Ohio State University, Columbus, Ohio 43210, United States

Dirk Wallacher

Berlin Neutron Scattering Center (BENS), Helmholtz-Zentrum Berlin für Materialien und Energie GmbH, Hahn-Meitner-Platz 1, D-14109 Berlin, Germany

**ABSTRACT:** The densities of pore-confined fluids were measured for the first time by means of vibrating tube densimetry (VTD). A custom-built high-pressure, high-temperature vibrating tube densimeter was used to measure the densities of propane at subcritical and supercritical temperatures (between 35 and 97 °C) and carbon dioxide at supercritical temperatures (between 32 and 50 °C) saturating hydrophobic silica aerogel (0.2 g/cm<sup>3</sup>, 90% porosity) synthesized inside Hastelloy U-tubes. Additionally, supercritical isotherms of excess adsorption for CO<sub>2</sub> and the same porous solid were measured gravimetrically using a precise magnetically coupled microbalance. Pore fluid densities and total adsorption isotherms increased monotonically with increasing density of the bulk fluid, in contrast to excess adsorption isotherms, which reached a maximum and then decreased toward zero or negative values above the critical density of the bulk fluid. The isotherms of confined fluid density and excess adsorption obtained by VTD contain additional information. For instance, the maxima of excess adsorption occur below the critical density of the bulk fluid at the beginning of the plateau region in the total adsorption, marking the end of the transition of pore fluid to a denser, liquidlike pore phase. Compression of the confined fluid significantly beyond the density of the bulk fluid at the same temperature was observed even at subcritical temperatures. The effect of pore confinement on the liquid–vapor critical temperature of propane was less than ~1.7 K. The results for propane and carbon dioxide showed similarity in the sense of the principle of corresponding states. Good quantitative agreement was obtained between excess adsorption isotherms determined from VTD total adsorption results and those measured gravimetrically at the same temperature, confirming the validity of the vibrating tube measurements. Thus, it is demonstrated that vibrating tube densimetry is a novel experimental approach capable of providing directly the average density of pore-confined fluids, and hence complementary to the conventional gravimetric or volumetric/piezometric adsorption techniques, which yield the excess adsorption (the Gibbsian surface excess).



### INTRODUCTION

The interest in processes involving supercritical fluids has increased significantly over the past two decades. An accurate description of the effects of fluid confinement is particularly important in the fields of supercritical separations, supercritical fluid chromatography, hydrogen and methane storage, enhanced coal bed methane recovery, natural gas recovery from deep shale formations, geologic sequestration of CO<sub>2</sub>, and geothermal heat mining using CO<sub>2</sub> instead of water. Experimental adsorption isotherms obtained over wider ranges of pressure extending to compressed liquid or dense supercritical fluid revealed effects that were not present or could be neglected in low-density gas adsorption. Most notably, the experimental adsorption isotherms show a maximum at the density of bulk fluid approaching its critical value.<sup>1–4</sup> At still

higher densities, experimental excess adsorption isotherms may reach zero or even negative values. This behavior is not caused by any additional volumetric effects, such as adsorbent swelling or deformation at elevated pressure. The decrease of the amount adsorbed with pressure may appear counterintuitive by implying a negative sign of the pressure derivative of density at constant temperature,  $(\partial Q/\partial P)_T$ , and hence mechanical instability of the system. However, the quantity measured by all conventional methods does not represent the total amount of fluid present in the vicinity of solid surface, but instead the excess adsorption (Gibbs surface excess). Excess adsorption,  $n_e$ ,

**Received:** November 15, 2011

**Revised:** February 24, 2012

**Published:** February 27, 2012

is the difference between the actual amount of fluid contained inside a pore system and the hypothetical amount of bulk fluid filling pore spaces, i.e., in the absence of fluid–solid interactions. For open surfaces the excess adsorption  $n_e$  is defined in terms of the density of the fluid  $\rho(r)$  at the distance  $r$  from the solid surface, and the bulk fluid density  $\rho_b$ , as

$$n_e = \int_0^{\infty} [\rho(r) - \rho_b] dr \quad (1)$$

Excess adsorption is the quantity accessible to most experimental adsorption methods, including conventional gravimetric and volumetric/piezometric measurements. In contrast, the absolute adsorption  $n_a$ , defined formally as

$$n_a = \int_0^l \rho(r) dr \quad (2)$$

depends on the thickness of the sorption layer  $l$ , which can be also interpreted as the extent of the potential field of the solid for a specific solid–fluid pair and at specific temperature and pressure conditions. The value of  $l$ , the distance from the surface beyond which  $\rho(r) = \rho_b$  for all  $r > l$ , cannot be determined exactly by experiment without additional assumptions. Therefore, in principle, also the absolute adsorption and the volume of the adsorbed phase cannot be uniquely determined.

The above is also true of the total adsorption  $n_t$ , defined for adsorption in pore systems as the sum of the absolute adsorption and the “unadsorbed” fraction of the fluid,  $n_u$ , which remains inside the pore system, but at distances greater than  $l$ , and thus not significantly affected by the potential field of the solid:

$$n_t = n_a + n_u \quad (3)$$

It follows from eqs 1 and 2 that the distinction between absolute adsorption and excess adsorption vanishes as the density of the bulk fluid approaches zero. Physical adsorption of vapors at temperatures well below the critical point or chemisorption of gases can approximate this condition accurately if the density of the gas phase is much lower than the density of the adsorbed phase. This reflects the traditional understanding of adsorption phenomena since the first experiments made over 200 years ago<sup>5</sup> as invariably associated with large drops of pressure caused by apparent condensation of the gas phase upon contact with a solid surface. Since the observed vapor-pressure-lowering effect caused by solid–fluid interactions could be interpreted as analogous to the effect of solute–solvent interactions causing clustering of solvent molecules around the solute, the same models have been sometimes used to describe both phenomena.<sup>6–8</sup> It was also often assumed that the average density of the sorbed phase was close to the density of the normal liquid under the conditions of “low pressure adsorption”.

However, the results of theoretical studies and simulations suggest that the properties of the adsorbed phase present in micropores or forming the first layers adhering to the surface can significantly depart from the properties of bulk liquid at equilibrium conditions. Additionally, the properties important to modeling the behavior of confined fluids, such as densities, phase transitions, heat capacities, and chemical potentials, are expected in general to vary as a function of distance from the interface. These effects become more important at high pressure, as the density of the bulk phase approaches the mean density of the confined phase. With increasing interest

and number of studies, considerable progress has been achieved in modeling of high-pressure adsorption and interpretation of experimental data, though challenges still remain.<sup>9–11</sup>

Excess adsorption, which can be measured without the knowledge of any microscopic properties of the adsorbed phase, is an important quantity used for thermodynamic analysis of many aspects of adsorption and is routinely utilized in modeling and control of technological processes.<sup>12</sup> However, the properties of the adsorbed phase, including the average density of the pore-filling fluid, are essential in development of some applications, such as, for example, supercritical fluid chromatography, determination of total sorptive capacity of porous media, and modeling of reactive fluid flow in geologic reservoirs. Pore-fluid density data are also needed for development and validation of new experimental methods such as small-angle neutron scattering (SANS), which is capable of probing local densities and structures of porous materials and pore fluids.<sup>13</sup>

In this paper we describe the first application of vibrating tube densimetry (VTD) to measurements of pore fluid density and total adsorption capacity in a mesoporous solid. In the vibrating tube method the porous solid completely fills the tube, so that virtually no bulk fluid outside of the pore system is present in the measurement zone; i.e., the contact with the bulk fluid reservoir occurs outside of the vibrating cantilever. The mass of the pore fluid, proportional to its average density, is measured directly as the inertia of the cantilever containing the solid sample imbedded with fluid.

One of the goals of this work is to investigate the effects of confinement on the properties of supercritical CO<sub>2</sub>, in particular those essential to geologic carbon sequestration and development of enhanced geothermal systems (EGS). Following the strategy delineated by Cole et al.,<sup>14</sup> this initial effort is focused on a well characterized engineered porous solid (silica aerogel) to facilitate comparison of the results with other experimental data and molecular-level computations. Propane was selected for the first measurements as a simple neutral fluid with a convenient temperature range of liquid–vapor equilibria ( $T_c = 96.7$  °C) and weak nonspecific interactions with silica. The deuterated propane/silica aerogel system was studied previously by means of SANS and neutron transmission.<sup>13</sup> Moreover, from the applied point of view, there is considerable interest in the sorption behavior of light hydrocarbons as well as carbon dioxide in rock formations with high quartz content, i.e., sandstone, shales, and other nanoporous geological materials.

## ■ EXPERIMENTAL SECTION

**Materials.** Hydrophobic supercritical-alcohol-dried monolithic silica aerogel used in the vibrating tube measurements was synthesized inside Hastelloy C22 U-tubes by Ocellus Technologies, Inc. (Livermore, CA). The silica aerogel exhibits an open structure of thin silica strands with mesh size between 7 and 9 nm (Figure 1). Monolithic blocks of aerogel obtained from the same source, with the same nominal density (0.2 g/cm<sup>3</sup>), were used in gravimetric adsorption measurements after crushing to 2–5 mm grain size. Using the skeletal density of the silica equal to 2.0 g/cm<sup>3</sup>,<sup>15,16</sup> the porosity of the samples was ~90%. The specific surface area of another sample of monolithic aerogel of the same density was determined by the classical multipoint BET nitrogen adsorption method. The averaged result obtained from four measurements was 307.3 m<sup>2</sup>/g with a standard deviation of 6.3 m<sup>2</sup>/g.

The grades and nominal purities of the gases used were as follows: propane (Matheson Tri Gas Research Purity, 99.993%); helium (Air

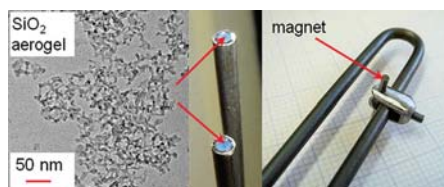


**Figure 1.** TEM image of the silica aerogel structure (silica strands are darker) and the Hastelloy U-tube with the silica gel synthesized inside and the magnet clamp attached.

Liquide Ultra High Purity, 99.999%); argon (Airgas Research Plus (for vibrating tube, 99.9999%) or Linde (for microbalance, 99.999%)), and carbon dioxide (Matheson Tri Gas Research grade (for vibrating tube, 99.999%) or Linde (for microbalance, 99.999%)).

**Methods.** *Vibrating Tube Densimeter.* High-pressure, high-temperature fluid flow vibrating tube densimeters were designed and custom built<sup>17,18</sup> at Oak Ridge National Laboratory for measurements of volumetric properties of pure and mixed fluids to 400 °C and 1000 bar. One of these instruments<sup>17</sup> was modified for novel measurements of confined fluid densities. The most important modification of the apparatus was the replacement of the existing U-tube (OD = 1.59 mm), previously welded to the supporting mount, with a new Hastelloy C-22 U-tube containing the porous solid (OD = 3.17 mm, ID = 1.78 mm; the length of the vibrating section = 90 mm). The U-tube with an Alnico V rod magnet attached to one of its arms (Figure 1) was clamped in a new Hastelloy mount designed to facilitate tube replacements. A steady baseline of the vibrational frequency of the evacuated U-tube (less than  $\pm 3$  ppm deviation over a period of several hours) confirmed strong adhesion of the aerogel to the tube. The pressure in the system was adjusted by means of a manual positive displacement pump (High Pressure Equipment Co., Model 112-5.75-5) and measured with two digital piezoresistive transducers calibrated by the manufacturer (Keller America, Inc.) with a maximum total error band of  $\pm 0.1\%$  of the full scale (345 and 552 bar). The temperature was measured with a platinum RTD and a digital thermometer (Instrulab Inc.) calibrated to an accuracy of  $\pm 0.02$  to 400 °C using fixed-point standards (the triple point of water and the freezing points of Sn and Zn) traceable to NIST. It was possible to control the temperature of the silver block housing the vibrating tube to within  $\pm 0.002$  K of the set point over periods of several weeks. Temperature, pressure, and vibration period data were continuously recorded every  $\sim 38$  s and plotted on the screen by a custom-made computer data acquisition program.

*Gravimetric Apparatus.* An automatic microbalance<sup>19,20</sup> (Rubotherm, Bochum, Germany) capable of mass resolution of 0.01 mg was used for weighing solid samples in a CO<sub>2</sub> atmosphere at 31.5, 32, 35, and 50 °C over the pressure range from vacuum to 200 bar. The principal advantage of the Rubotherm balance is its electromagnetic suspension of the adsorbent sample, allowing for a complete isolation of the sorptive fluid from the mechanism of the balance, and thus permitting work with corrosive and/or condensable gases at high pressure and temperature. The Rubotherm apparatus was used without modification. The stainless steel basket holding the sample ( $\sim 0.9$  g) was located inside a thermostated stainless steel cylindrical pressure vessel. An electrical heating jacket kept the pressure vessel enclosing the sample at within  $\pm 20$  mK of the set point temperature. As with the VTD apparatus, a manual positive-displacement pump (High Pressure Equipment Co.) was used to store and pressurize the fluid. The pressure of the fluid surrounding the sample was increased manually for each equilibration and was measured with a digital piezoresistive gauge accurate to 0.1% and calibrated by the manufacturer (Keller America, Inc.). It usually took 30–60 min to reach thermal and mass transfer equilibria after each change of the pressure of CO<sub>2</sub>. Weighing cycles were executed by the software provided by the manufacturer automatically and continuously, one after another, approximately every

10 s. Each weighing cycle consisted of two steps: (i) the calibration/taring step, with the sample basket decoupled from the balance, and (ii) the actual measurement of the force required to suspend the sample. Before starting each isotherm the pressure vessel was evacuated by means of a two-stage turbomolecular pump capable of providing vacuum of  $10^{-2}$  mbar or better. The results of weighing, corrected for the effect of buoyancy in CO<sub>2</sub>, represent excess adsorption isotherms. The required densities of CO<sub>2</sub> were calculated using the NIST REFPROP 9 software<sup>21</sup> based on an accurate equation of state for bulk carbon dioxide.<sup>22</sup>

## RESULTS AND DISCUSSION

Vibrating tube fluid densimetry is based on the linear dependence of the square of the vibration period of a uniform cantilever on its density. The cantilever is formed by a U-shaped tube containing the fluid under investigation and vibrating in the direction orthogonal to the plane of the tube. In principle, the vibration period  $\tau$  can be determined from the known geometry and mechanical properties of the cantilever. However, in practice, the most accurate results are obtained by calibration with reference fluids using equations of state. The difference between the unknown density  $\rho$  and the reference fluid density  $\rho_0$  is given by

$$\rho - \rho_0 = K(\tau^2 - \tau_0^2) \quad (4)$$

where  $\tau$  and  $\tau_0$  are the vibration periods of the fluid under investigation and the reference fluid, respectively. The slope  $K$  can be determined using at least two reference fluids. Vacuum can be substituted for one of the reference points, if the effect of deformation of the vibrating tube caused by pressure can be neglected. Measurements of the density of confined helium at 35 °C demonstrated that the effect of pressure up to 100 bar on the vibration frequency was not detectable. Assuming also negligible adsorption of helium in silica aerogel, this result indicates a negligible pressure effect on the relatively rigid, heavy-walled tubing used. Accordingly, the vibration period at each temperature of the evacuated tube filled with the aerogel was used as one of the reference points.

Past experience shows that the deviation of eq 4 from linearity is negligible in comparison with other sources of error, so that there is no need to calibrate with more than two fluids or use more complex nonlinear calibration equations. This is due to (i) nearly ideal harmonic vibrations assured by the small amplitude in comparison with the cantilever length and (ii) relatively small changes of the mass of the cantilever and consequently relatively small changes in the oscillation frequency. The linearity of eq 4 coupled with very accurate measurement of time (frequency) make possible the high accuracy that can be achieved using the vibrating tube method. The vibration frequency of the evacuated tube filled with silica aerogel was about 263 Hz, and the frequency decrease due to saturation with CO<sub>2</sub> at 35 °C and 139 bar (bulk fluid density of  $\sim 0.8$  g/cm<sup>3</sup>) was  $\sim 4$  Hz. The periods of vibration ( $\sim 3.8$  ms) were averaged over  $\sim 38$  s intervals and recorded continuously with the resolution of 1 ns (seven digits).

Obtaining quantitative results from vibrating tube measurements of confined fluid densities is not as straightforward as in the case of bulk fluids because there are no pore-confined fluid density standards. In this work we used the results for helium, propane, and argon at 35 °C, as interpreted below, to calibrate the vibration period data and obtain absolute values of confined fluid density. The analysis of the isotherms indicated that (i) excess adsorption in silica aerogel of inert gases, such as He and

Ar at 35 °C, far above their critical temperatures, is negligible and (ii) the average densities of fluids confined in silica aerogel approach the bulk fluid density at high pressure. Additionally, the slope  $K$  in eq 4 was also calculated using geometrical and mechanical properties of the vibrating cantilever and compared to the value obtained by calibration.

**Calibration of the VTD Using Propane and Argon at 35 °C.** Figure 2 shows the densities of confined propane

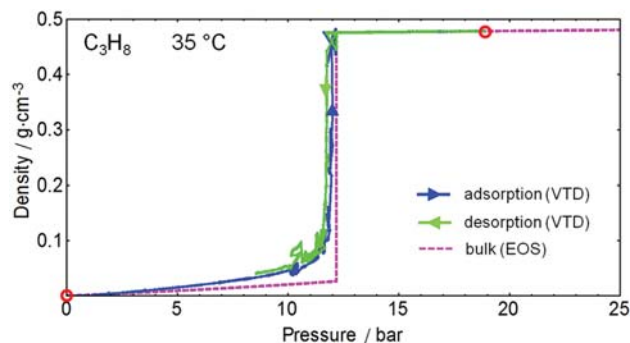


**Figure 2.** Measured densities of confined and bulk propane at 35 °C. The circles indicate the points used to determine the slope  $K$  in eq 4 (at vacuum and at  $P = 19$  bar, where the densities of confined and bulk fluids are assumed to be equal).

measured at pressures between vacuum and 19 bar during adsorption and desorption at 35 °C. Also shown in Figure 2 is the density of bulk propane.<sup>21,23</sup>

The vibration period vs density slope  $K$  of eq 2 was determined by assuming that at 35 °C and at  $P \sim 19$  bar the densities of confined and bulk propane are equal (and, of course, both are zero at vacuum). If  $K$  is selected so that the measured density of the pore liquid is equal to that of bulk propane at these conditions, the compressibilities (the slopes of the high-pressure sections of the isotherms) are also identical, as shown in Figure 2. Note that the shape of the low-pressure section of the confined fluid isotherm in Figure 2 suggests that at 35 °C, well below the critical point, the pore fluid begins to condense to a much denser phase at a pressure significantly lower than the saturation pressure  $P_s$  of the bulk fluid ( $P_s = 12.18$  bar, marked by the vertical section of the bulk fluid isotherm). However, most fluid condenses at pressures only slightly lower than  $P_s$  and the condensation in the largest pores is complete at a pressure very close to  $P_s$ .

The calibration of eq 4 based on the density of subcritical liquid pore propane was confirmed by the results for argon adsorption at 35 °C. Figure 3 shows the density isotherm for argon corresponding to Figure 2 for propane.

The vibration period data for Ar were converted to densities using the value of  $K$  determined from the propane data as described above. In Figure 3, the resulting slope of the density of pore-confined argon as a function of pressure, which depends on the value of  $K$ , is the same as that of bulk argon.<sup>21,24</sup> This indicates that excess adsorption on silica aerogel was negligible at the temperature nearly 160 K above the critical temperature ( $T_c = -122.46$  °C for Ar). The absolute difference between bulk and confined densities visible in Figure 3 (less than  $0.03$  g/cm<sup>3</sup>) is most likely an experimental artifact. Specifically, the baselines at vacuum measured for different isotherms were subject to random shifts of up to  $\pm 0.06$  g/cm<sup>3</sup> over periods of several days. The reason for the significantly

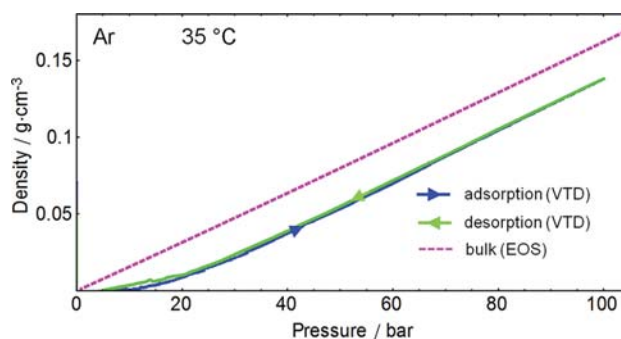


**Figure 3.** Measured density of pore-confined argon compared with bulk gas density.

smaller slope of the measured confined fluid isotherm relative to the bulk fluid visible in Figure 3 at low densities (to  $0.02$  g/cm<sup>3</sup>) is currently not clear but under investigation.

While the results for argon and those for propane and carbon dioxide at other temperatures discussed below support this method of calibration, there is no guarantee that the same assumptions will necessarily be valid for every combination of porous solid and fluid adsorptive. In materials characterized as significantly microporous, the pore fluid is on average in closer proximity to the solid–fluid interface, while in contrast, the contact between the confined and bulk phases is weaker. For this reason the average properties of the confined fluid phase in micropores may be affected to a greater degree by the interfacial forces and less by the equilibrium with the bulk fluid. In such systems the density difference between confined and bulk fluid could persist to higher pressures. Additionally, the filling of molecular size pores can be affected by the size and geometry of the fluid molecules. As a consequence, further experiments with microporous solids are needed to verify the calibration of eq 4 by the methods described above. Nevertheless, even if accurate absolute values of pore fluid density could not be obtained from calibration using reference fluids, vibrating tube densimetry would still provide valuable information on the relative changes of the density of the confined fluids with pressure, fluid phase transitions, and relative densities for different fluids. In addition, absolute densities can be also obtained by calculation of the resonance frequency from the geometry and mechanical properties of the vibrating tube, as described below.

**Estimation of the Vibration Period Using the Mechanical Properties of a Vibrating Cantilever.** For an evacuated cantilever tube ( $Q_0 = 0$ ) the slope  $K$  in eq 4 can be calculated from<sup>25</sup>

$$K = \left( \frac{n^2}{2\pi L} \right)^2 \frac{EI}{V_{\text{pore}}} \quad (5)$$

where  $L$  is the length of the cantilever,  $E$  is the Young's modulus of elasticity for Hastelloy C22,  $I$  is the second moment of the tube cross-section area,  $I = \pi/64(\text{OD}^4 - \text{ID}^4)$ ,  $V_{\text{pore}}$  is the volume of the pore space per unit length of the cantilever, and  $n$  is the characteristic constant for the principal mode of vibration ( $n = 1.8751$ ). The vibration period  $\tau_0$  of the tube filled with porous solid and evacuated is then

$$\tau_0 = \sqrt{\frac{m_0}{KV_{\text{pore}}}} \quad (6)$$

where  $m_0$  is the mass of the tube containing the porous solid per unit length of the cantilever. The remaining symbols have the same meanings as defined above.

The data used for calculation of  $K$  and  $\tau_0$  from eqs 5 and 6 included nominal outer and inner diameters of the tubing, the typical Young's modulus for Hastelloy C22, the measured length of the U-tube, the weighed masses of empty and solid-filled tubes, and the pore volume determined from the difference. A correction was applied for the additional point mass of the magnet and its titanium mount located about 24 mm from the free end of the cantilever (cf. Figure 1). The parameters of eq 4, obtained from the calibration using liquid propane and the calculation as described above, are summarized in Table 1.

**Table 1. Parameters of Eq 3 from Calibration and Calculation**

	calibrated	calculated	difference (%)
$K$ ( $\text{g cm}^{-3} \text{ms}^{-2}$ )	1.713	1.876	+10
$\tau_0$ (ms)	3.805	3.470	-10

The agreement between the two methods is quite satisfactory, taking into account the approximations involved. The end effect of the U-tube was neglected, and the nominal tubing dimensions and Young's modulus  $E$  were used. The contribution of the aerogel to the rigidity (but not the mass) of the Hastelloy tube was neglected. A more accurate determination of the calibration equation parameters could be made in the future through an experimental characterization of the mechanical properties of the empty cantilever U-tube using reference fluids.

**Pore Fluid Densities and Isotherms of Total Adsorption for  $\text{C}_3\text{H}_8$  and  $\text{CO}_2$ .** The measurements of the densities of pore propane were made at four subcritical temperatures (35, 70, 92, and 95 °C) and at 97.0 °C, about 0.3 K above the critical temperature ( $T_c = 96.7$  °C). A summary of the proof-of-principle experiments for the VTD method is shown in Figure 4, where the measured densities of the pore fluid are plotted as

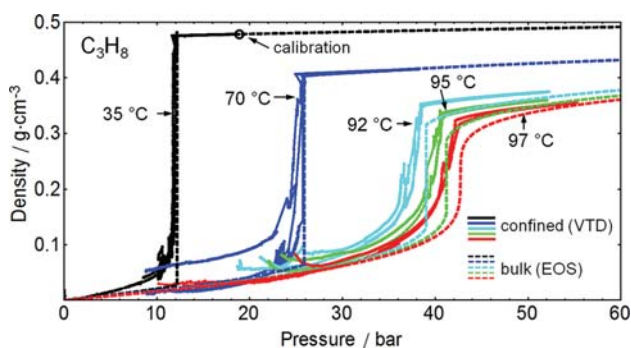


**Figure 4.** Subcritical (35, 70, 92, and 95 °C) and supercritical (97 °C) isotherms of confined fluid density for propane in silica aerogel.

a function of pressure together with the densities of the bulk fluid calculated from the equation of state.<sup>21,23</sup>

The pore fluid densities were calculated for all temperatures using eq 4 and the “calibrated” value of the parameter  $K$  listed in Table 1. The temperature coefficient of  $K$  was found to be small, so that a good representation of the experimental results was obtained between 35 and 97 °C using the same value of  $K$

which was determined for liquid propane at 35 °C. As indicated by the higher temperature isotherms in Figure 4, more accurate values of  $K$  could be obtained for each isotherm using VTD results extended to higher pressures, where confined and bulk fluid densities and compressibilities are expected to converge.

In contrast to  $K$ , the temperature coefficient of the vibration period at vacuum was significant. It was determined from all available results at constant densities as  $5 \pm 0.3 \mu\text{s/K}$ , valid in the pressure range from vacuum to  $\sim 200$  bar. The vibration periods at vacuum,  $\tau_0$  in eq 4, were either measured directly at each temperature or calculated using the linear dependence of the vibration period on temperature.

The isotherms plotted in Figure 4 show that the value of  $K$  determined at one temperature (35 °C) produced a consistent relationship between the pore fluid and bulk fluid densities at all higher temperatures. All isotherms feature a region of steep density increase corresponding to the vapor–liquid phase transition (pore condensation). As the pressure increases, this phase transition begins in the smallest pores in a range of pressures below the saturated vapor pressure of the bulk fluid, without a clearly defined onset pressure. In contrast, the end of the transition, which may be interpreted as complete filling of the widest pores, is well-defined at all temperatures, including the slightly supercritical 97 °C adsorption/desorption isotherms. This behavior is in agreement with the dependence of vapor pressure lowering on pore size observed in many porous adsorbents and predicted by the Kelvin equation for classical capillary condensation.

The confined fluid density isotherms in Figure 4 exhibit a significant contrast between the large spikes visible at lower pressures, and the smooth curves in the region corresponding to compressed liquid, with a tight overlap of the adsorption and desorption branches. To understand this difference, it is important to take into account that (i) the large scatter of the isotherms occurs in the two-phase region, where the effective compressibility of the fluids is very large, and (ii) during the measurements the pressure was increased or decreased manually at a very slow rate (it took 2–4 weeks to obtain a complete adsorption/desorption isotherm). Even very small variation of pressure, unavoidable, e.g. overnight, and also resulting from stepwise pressure changes, would cause significant shifts of the fraction of the fluid condensed in the smaller pores. The reasons for adopting this rather slow procedure was primarily to prevent the anticipated possible damage to the aerogel caused by rapid condensation/evaporation in the pores (accompanied by large volumetric and thermal effects) but also to validate complete thermodynamic equilibrium by comparing results obtained at different rates of pressure change. Although the results of both VTD and gravimetric measurements indicated that the kinetics of adsorption and diffusion were fast enough to allow a much faster rate of pressure scanning, we still cannot rule out possible damage (e.g., microcracking) to the aerogel inside vibrating tube caused by rapid changes of fluid pressure. While the gravimetric adsorption isotherms were obtained in only several hours, the mechanical integrity of the adsorbent is not as important to this method as it is to VTD, for obvious reasons.

In summary, the scatter observed in the two-phase region (Figure 4, at lower pressures) was caused by the inherent instability of the relative amounts of two phases in equilibrium. This effect would also occur (and indeed has been observed) during VTD measurements of bulk fluid densities. The resulting peaks represent real fluctuations of the mean density

of the pore fluid, not a fault of the instrument. This behavior has never been observed for either propane or CO<sub>2</sub> at the conditions where only one phase was expected (e.g., significantly above the critical temperature or at high pressure).

At 35 and 70 °C, in the bulk compressed liquid region, the densities and the compressibilities of the pore fluid and the bulk fluid are equal within the limits of experimental accuracy. However, this is no longer true at temperatures above 90 °C. At the highest three temperatures in Figure 4 the densities of the pore fluid are considerably higher and its compressibilities are considerably lower than those of the bulk fluid. Nevertheless, as the pressure increases further, the densities of the pore and bulk fluids appear to converge in the pressure range investigated, supporting the hypothesis that for this system the average pore fluid becomes similar the bulk liquid at a sufficiently high pressure.

The isotherms shown in Figure 4 support the findings of Aranovich and Donohue,<sup>26–28</sup> who identified a new phenomenon of “adsorption compression”. On the basis of a theoretical analysis of monolayer adsorption, Monte Carlo simulations, and calorimetric data on compressible gas adsorption, they concluded that the densities of the adsorbed phase may significantly exceed the density of the bulk liquid phase—an effect not taken into account in the earlier experimental and theoretical approaches to adsorption. The VTD results shown in Figure 4 suggest that this effect should be the greatest for highly compressible fluids and strong solid–fluid interactions, but negligible far below the critical temperature, where the compressibility of the liquid phase is too low for the interfacial forces to significantly compress it further. Conversely, as the compressibility of the pore fluid increases with increasing temperature, the surface field becomes sufficiently strong to compress the confined phase well beyond the density of bulk liquid at the same pressure. For example, the isothermal compressibility of liquid propane at the saturation pressure and at  $T = 95$  °C is much greater than the same property at  $T = 35$  °C (by a factor of 174) or  $T = 70$  °C (by a factor of 46). A magnified view of the 95 °C isotherms for propane is shown in Figure 5, where the density difference between the pore fluid and the bulk fluid is marked as  $\Delta\rho$ .

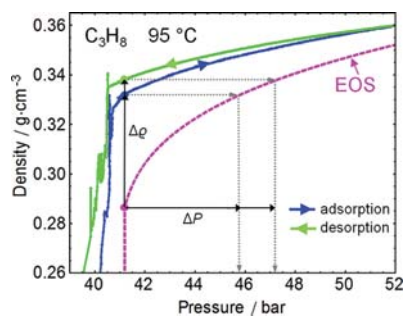


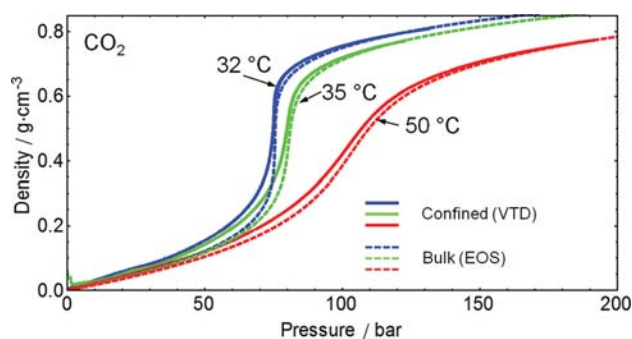
**Figure 5.** The 95 °C confined and bulk fluid density isotherms for propane showing the compression of the confined phase relative to bulk liquid at the same pressure.

At the saturated vapor pressure  $P_s = 41.2$  bar, the density of liquid propane is 0.2865 g/cm<sup>3</sup> while the measured densities of the confined phase, marked in Figure 5, are 0.332 g/cm<sup>3</sup> (adsorption) and 0.338 g/cm<sup>3</sup> (desorption). The equivalent pressures required to compress bulk liquid propane to these densities are 45.8 bar (adsorption) and 47.3 bar (desorption).

Therefore, in this example, the confined fluid compression caused by the interfacial forces is equivalent to the compression of the bulk liquid caused by pressure increases by  $\Delta P = 4.6$  bar (adsorption) or  $\Delta P = 6.1$  bar (desorption). The results shown in Figure 5 can be interpreted as direct experimental evidence of the compression of pore fluid induced by solid–fluid interactions. For other adsorbent/adsorbate pairs the magnitude of this effect will clearly depend on the strength of solid–fluid interactions, pore system features, and fluid properties.

It should be noted that at pressures lower than the point of complete filling of the pores with the liquidlike phase (in Figure 5,  $\sim 41$  bar for adsorption and  $\sim 40.5$  bar for desorption) a lighter, gaslike phase is also present in the larger pores. Therefore, at these conditions the measured density of the pore fluid is a mean value of the two phases, depending mainly on their relative volumes. As a consequence, in this region, the measured difference between the corresponding pore fluid and bulk fluid densities obviously does not reflect the phenomenon of “adsorption compression”. As an exception to this rule, a limited (up to  $\sim 1$  bar) persistence of the (metastable) dense liquidlike phase into the lower pressure two-phase region was observed in the desorption isotherms at 35 and 70 °C.

The observed decrease of the confinement effect on the density of the relatively incompressible pore fluid well below the critical temperature provided the means for calibrating our VTD measurements as described above. For the same reason the confinement effect vanishes at high pressure, as the density of the confined fluid converges to the density of bulk fluid from above (Figure 4). At a sufficiently high pressure, as the compressibility of the supercritical fluid becomes comparable to that of the normal liquid, the surface force field again may be too weak to significantly affect the average density of the pore fluid.



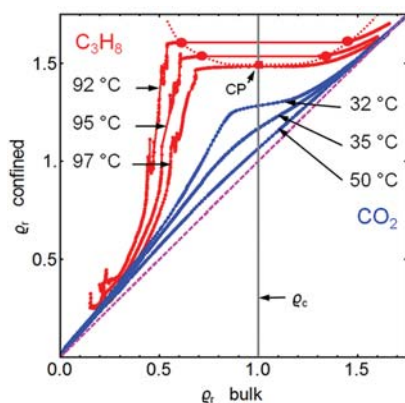
**Figure 6.** Supercritical (32, 35, and 50 °C) isotherms of confined and bulk fluid density for carbon dioxide in silica aerogel.

Figure 6 shows confined fluid density isotherms for supercritical carbon dioxide at 32, 35, and 50 °C (bulk CO<sub>2</sub> critical temperature  $T_c = 31.0$  °C).

The densities of bulk fluid at each temperature were calculated from the equation of state.<sup>21,22</sup> Again, the same slope  $K$  was used for eq 4 as determined for propane at 35 °C and listed as “calibrated” in Table 1. The results for propane and CO<sub>2</sub> are consistent; the densities and compressibilities of the pore-confined and bulk fluids converge at high pressure. In contrast to propane, practically no hysteresis was observed for

supercritical CO<sub>2</sub>, so that the adsorption and desorption isotherms overlap in Figure 6 over the entire pressure range.

The total average densities of the confined fluids measured by VTD and shown in Figures 4 and 6 are monotonically increasing functions of the pressure (or density) of the bulk fluid. To compare the results for propane and carbon dioxide, and emphasize the corresponding states similarity between the two fluids, the results are shown in Figure 7 in terms of reduced densities  $Q_r = Q/Q_c$  where  $Q_c = 0.220 \text{ g/cm}^3$  for C<sub>3</sub>H<sub>8</sub> and  $Q_c = 0.4676 \text{ g/cm}^3$  for CO<sub>2</sub>.



**Figure 7.** Total confined fluid reduced density isotherms for C<sub>3</sub>H<sub>8</sub> and CO<sub>2</sub> plotted as a function of bulk fluid reduced density.

The diagonal dashed straight line in Figure 7 represents the hypothetical condition where the confined fluid density is equal to the bulk fluid density; the deviations of the experimental isotherms from this line represent the excess density due to solid–fluid interactions, shown in Figure 8, and also as excess adsorption for CO<sub>2</sub> in Figure 9.

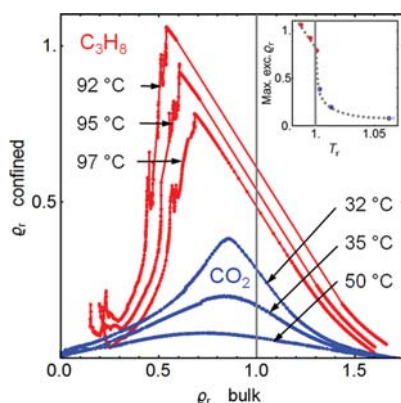


**Figure 8.** Excess confined fluid density isotherms for C<sub>3</sub>H<sub>8</sub> and CO<sub>2</sub> corresponding to the total adsorption isotherms in Figure 7. The inset is a plot of the maxima of the excess densities for propane and CO<sub>2</sub> as a function of reduced temperature.

Figure 7 demonstrates that the confined fluid densities, and consequently total adsorption isotherms, are nondecreasing functions of increasing bulk fluid density. Each of the subcritical isotherms features a plateau formed by a straight tie line extending between the densities of bulk vapor and liquid phases in equilibrium. The dotted curve in Figure 7 represents the vapor–liquid equilibrium envelope of bulk propane with the

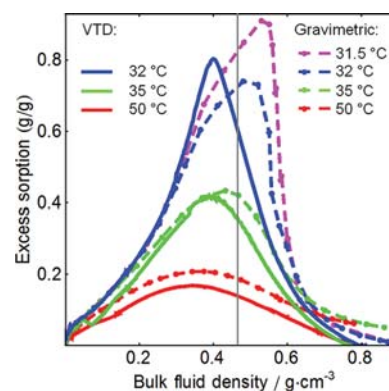


**Figure 9.** Excess adsorption isotherms for CO<sub>2</sub> obtained by VTD (continuous curves) and gravimetrically (dashed curves and symbols). The vertical line marks the critical density of CO<sub>2</sub> (0.4676 g/cm<sup>3</sup>).

densities of the phases in equilibrium at each temperature and the bulk fluid critical point marked with symbols. In the isotherms exceeding the critical temperature (starting from the 97 °C isotherm for propane shown in Figure 7) the horizontal tie line is replaced by a segment representing the vestige of the vapor–liquid equilibrium in the supercritical region, with the slope which is initially flat, but which becomes increasingly positive with increasing temperature. At the same time the maximum deviation of the confined fluid density from the bulk fluid density decreases with increasing temperature. The excess densities corresponding to the total density isotherms shown in Figure 7 are plotted in Figure 8.

The inset in Figure 8 shows the maxima of the excess density isotherms for both propane and CO<sub>2</sub> as a function of reduced temperature. The apparently continuous evolution with temperature of the pore fluid density isotherms for propane and carbon dioxide demonstrates the similarity of these two confined fluids, in agreement with the principle of corresponding states. This observation is consistent with relatively weak interactions of both fluids with the solid matrix. Note that, according to the law of rectilinear diameters, the critical density (reduced density  $Q_{rc} = 1$ ) should be located close to the center of the plateau regions in Figure 7 or close to the center of the corresponding decreasing sections in the excess density isotherms in Figure 8. As a consequence, the maxima of excess adsorption appear at densities significantly lower than the critical density, at least at subcritical and not too high supercritical temperatures.

**Excess Adsorption Isotherms Obtained by VTD and Gravimetric Methods.** Figure 9 shows the VTD results for CO<sub>2</sub> plotted as excess adsorption isotherms together with the corresponding isotherms measured directly by means of the automatic electromagnetically coupled microbalance described above.

Figure 9 shows excess adsorption isotherms for CO<sub>2</sub> obtained by both methods at three temperatures: 32, 35, and 50 °C. Additionally, the 31.5 °C isotherm is shown only for the gravimetric method. The nominal specific pore volume (pore volume per gram of adsorbent) of 4.5 cm<sup>3</sup>/g was used to convert the density difference between confined and bulk fluid obtained from the VTD results to the excess adsorption expressed as a fluid to solid mass ratio plotted on the vertical axis in Figure 9. The same specific pore volume was also used to calculate the buoyancy correction to the gravimetric data. This value is based on the nominal density of the silica aerogel

(0.2 g/cm<sup>3</sup>) and the skeletal density of the silica particles. The value of 2.0 g/cm<sup>3</sup> was accepted for the latter, based on helium pycnometry results.<sup>15,16</sup> Such measurements were not made for the aerogel samples used in this work, and therefore, taking into account the variation of literature data for various silica aerogel samples, the absolute accuracy of the specific pore volume is not expected to be better than 10%.

The quantitative agreement between the three pairs of isotherms measured by each of the two methods is very satisfactory. The most visible difference between VTD and gravimetric results is the location of the isotherm maxima. As discussed above, the analysis of the subcritical and supercritical isotherms of total density indicates that the maxima of excess adsorption should fall appreciably below the critical density of bulk fluid. However, the maximum of the gravimetric isotherm of excess adsorption at 32 °C occurs just above the critical density, and the maximum at 31.5 °C occurs at a density even higher. The question whether this difference is caused by experimental error or it originates from the inherent differences between the two techniques deserves further experimental and theoretical analysis. One of possible effects which will require additional investigation is possible adsorbent expansion/contraction caused by both pressure variation and interaction of the solid with the sorbed fluid.<sup>28</sup>

## CONCLUSION

It has been demonstrated that vibrating tube densimetry can be used to obtain a unique insight into the properties of fluids confined in pore systems. On the basis of the proof-of-principle experiments reported in this paper, we anticipate that the VTD method can become an important tool for investigation of high-pressure adsorption, complementary to other experimental and theoretical approaches. A comparison of excess adsorption isotherms derived from VTD with those obtained gravimetrically for CO<sub>2</sub>/silica aerogel (Figure 9) validated the experimental procedure and the assumptions used in this work to calibrate the equipment and obtain quantitative results.

One porous solid and two fluids were included in this initial study, but the new technique can be applied to a wide range of different adsorbate/adsorbent pairs. The properties of pore systems vary widely even among silica aerogels with different densities and methods of preparation. In addition, the strength of interactions at the interface depends on the physical and chemical properties of both fluids and solids. However, the results of this work may allow for some universal insight into high-pressure sorption behavior. In the systems characterized by relatively weak and nonspecific interactions, such as hydrophobic silica aerogels with pores in the mesopore range and nonpolar fluids, the state of the confined fluid is the result of competition between equilibria with the bulk fluid on one side and the solid surface on the other. In the case of an open system of relatively wide pores, while the properties of the fluid in direct vicinity of the interface are affected the most, the mean properties of the pore fluid are not entirely different from the bulk fluid. In agreement with literature descriptions<sup>29,30</sup> of adsorption regimes resembling, at least phenomenologically, classical capillary condensation, the present results also support the concept of separation of pore fluid into two phases, similar to liquid–vapor equilibrium in bulk fluid. As the densities and phase transition points of the confined phases are altered by the surface force field, additional phase transitions may occur, and the properties of the phases can vary locally, e.g. with the pore

size, but the general distinction between the liquidlike and vaporlike phases remains realistic.

The isotherms shown in Figure 7 indicate that the depression of the liquid–vapor critical temperature of confined propane relative to bulk propane ( $T_c = 96.7$  °C) is less than ~1.7 K. This conclusion is supported by the shape of the isotherms at 95 °C and lower temperatures clearly indicating phase equilibrium, in contrast to the supercritical isotherms (97 °C for propane and all three isotherms for CO<sub>2</sub>). Additional isotherms between 95 and 96.7 °C could provide a more accurate determination of the magnitude of the finite size effect on the critical temperature. Significantly greater effects of confinement on the critical point, based on hysteresis phase diagrams, have been measured for other confined systems, e.g., over 40 K for CO<sub>2</sub> in Vycor glass.<sup>31,32</sup>

It should be expected that for solids characterized by sufficiently small uniform pores, at pressures above that required for complete pore filling with the liquidlike phase, almost all of the pore fluid would be affected by surface forces. Accordingly, for substantially microporous solids, the entire pore volume may be a reasonable definition of the extent of the potential field of the solid.<sup>9</sup> In such a model, the upper limit of the integral in eq 2 can be replaced by the pore size and the amount of unadsorbed fluid  $n_u$  in eq 3 is zero.

The results for propane shown in Figures 4 and 5 represent direct experimental evidence that the average density of the confined liquidlike phase can significantly exceed the density of normal bulk liquid, even if fluid–solid interactions are relatively weak. This densification effect has been compared to the densification of air in the gravitational field of the Earth.<sup>27,30</sup> However, for systems similar to those studied here, the effect of the solid surface field on the average density of the confined fluid is expected to virtually vanish at temperatures sufficiently below critical, or at pressures sufficiently above critical, in both cases due to the decreasing compressibility of the fluid under these conditions. Further VTD measurements for adsorbents with varying pore sizes will provide additional information on the effect of average distance from the interface on the properties of the confined fluid. The full potential of this approach will be realized by extending confined fluid density measurements to a range of porous materials with different chemistries and pore systems in conjunction with other methods, including gravimetric and small-angle neutron scattering (SANS). We also anticipate future application of a flow-through VTD technique to adsorption of mixed fluids.

## AUTHOR INFORMATION

### Corresponding Author

\*E-mail: gruszkiewicz@ornl.gov.

### Notes

The authors declare no competing financial interest.

## ACKNOWLEDGMENTS

We thank Dr J. M. Simonson for providing vital information on the construction and operation of the original VTD apparatus. This material is based upon work supported as part of the Center for Nanoscale Control of Geologic CO<sub>2</sub>, an Energy Frontier Research Center funded by the U.S. Department of Energy, Office of Science, Office of Basic Energy Sciences. The contribution of D.J.W. was sponsored by the Division of Chemical Sciences, Geosciences and Biosciences, Office of Basic Energy Sciences, U.S. Department of Energy.

## ■ REFERENCES

- (1) Parcher, J. F.; Strubinger, J. R. *J. Chromatogr.* **1989**, *479*, 251–259.
- (2) Strubinger, J. R.; Parcher, J. F. *Anal. Chem.* **1989**, *61*, 951–955.
- (3) Aranovich, G. L.; Donohue, M. D. *J. Colloid Interface Sci.* **1998**, *200*, 273–290.
- (4) Donohue, M. D.; Aranovich, G. L. *Fluid Phase Equilib.* **1999**, *158–160*, 557–563.
- (5) Gregg, S. J.; Sing, K. S. W. *Adsorption, Surface Area and Porosity*, 2nd ed.; Academic Press: London, U.K., 1982; Chapter 1.
- (6) Subramanian, R.; Lira, C. T. *Ind. Eng. Chem. Res.* **1995**, *34*, 3830–3837.
- (7) Humayun, R.; Tomasko, D. L. *AIChE J.* **2000**, *46*, 2065–2075.
- (8) Ally, M. R. *J. Chem. Eng. Data* **2009**, *54*, 411–416.
- (9) Myers, A. L.; Monson, P. A. *Langmuir* **2002**, *18*, 10261–10273.
- (10) Jakubov, T. S.; Jakubov, E. S. *Colloid J.* **2007**, *69*, 666–670.
- (11) Zhou, Y.; Zhou, L. *Langmuir* **2009**, *25*, 13461–13466.
- (12) Sircar, S. *Ind. Eng. Chem. Res.* **1999**, *38*, 3670–3682.
- (13) Rother, G.; Melnichenko, Y. B.; Cole, D. R.; Frielinghaus, H.; Wignall, G. D. *J. Phys. Chem. C* **2007**, *111*, 15736–15742.
- (14) Cole, D. R.; Chialvo, A. A.; Rother, G.; Vlcek, L.; Cummings, P. T. *Philos. Mag.* **2010**, *90*, 2339–2363.
- (15) Woignier, T.; Phalippou, J. *J. Mater. Sci.* **1990**, *25*, 3118–3126.
- (16) Tajiri, K.; Igarashi, K.; Nishio, T. *J. Non-Cryst. Solids* **1995**, *186*, 83–87.
- (17) Simonson, J. M.; Oakes, C. S.; Bodnar, R. J. *J. Chem. Thermodyn.* **1994**, *26*, 345–359.
- (18) Blencoe, J. G.; Drummond, S. E.; Seitz, J. C.; Nesbitt, B. E. *Int. J. Thermophys.* **1996**, *17*, 179–190.
- (19) De Weireld, G.; Frère, M.; Jadot, R. *Meas. Sci. Technol.* **1999**, *10*, 117–126.
- (20) Pini, R.; Ottiger, S.; Rajendran, A.; Storti, G.; Mazzotti, M. *Adsorption* **2006**, *12*, 393–403.
- (21) Lemmon, E. W.; Huber, M. L.; McLinden, M. O. NIST Standard Reference Database 23: Reference Fluid Thermodynamic and Transport Properties-REFPROP, Version 9.0, National Institute of Standards and Technology, Standard Reference Data Program, Gaithersburg, MD, 2010.
- (22) Span, R.; Wagner, W. *J. Phys. Chem. Ref. Data* **1996**, *25*, 1509–1596.
- (23) Lemmon, E. W.; McLinden, M. O.; Wagner, W. *J. Phys. Chem. Ref. Data* **2009**, *54*, 3141–3180.
- (24) Tegeler, C.; Span, R.; Wagner, W. *J. Phys. Chem. Ref. Data* **1999**, *28*, 779–850.
- (25) Stokey, W. F. In *Harris' Shock and Vibration Handbook*, 5th ed.; Harris, C. M., Piersol, A. G., Eds.; McGraw-Hill: New York, 2002; Chapter 7.
- (26) Aranovich, G. L.; Donohue, M. D. *Colloids Surf., A* **2001**, *187–188*, 95–108.
- (27) Aranovich, G. L.; Donohue, M. D. *Langmuir* **2003**, *19*, 2722–2735.
- (28) Aranovich, G. L.; Donohue, M. D. *J. Colloid Interface Sci.* **2005**, *292*, 202–209.
- (29) Detcheverry, F.; Kierlik, E.; Rosinberg, M. L.; Tarjus, G. *Phys. Rev. E* **2003**, *061504–1–061504–12*.
- (30) Ciccariello, S.; Melnichenko, Y. B.; He, L. *J. Appl. Crystallogr.* **2011**, *44*, 43–51.
- (31) Burgess, C. G. V.; Everett, D. H.; Nutall, S. *Pure Appl. Chem.* **1989**, *61*, 1845–1852.
- (32) Gelb, L. D.; Gubbins, K. E.; Radakrishnan, R.; Sliwinska-Bartkowiak, M. *Rep. Prog. Phys.* **1999**, *62*, 1573–1569.